

Non-resonant kaon pair production and medium effects in proton–nucleus collisions

This content has been downloaded from IOPscience. Please scroll down to see the full text.

2015 J. Phys. G: Nucl. Part. Phys. 42 075107

(<http://iopscience.iop.org/0954-3899/42/7/075107>)

View [the table of contents for this issue](#), or go to the [journal homepage](#) for more

Download details:

IP Address: 134.94.181.41

This content was downloaded on 03/06/2015 at 17:03

Please note that [terms and conditions apply](#).

Non-resonant kaon pair production and medium effects in proton–nucleus collisions

E Ya Paryev^{1,2}, M Hartmann³ and Yu T Kiselev²

¹Institute for Nuclear Research, Russian Academy of Sciences, Moscow 117312, Russia

²Institute for Theoretical and Experimental Physics, Moscow 117218, Russia

³Institut für Kernphysik and Jülich Centre for Hadron Physics, Forschungszentrum Jülich, D-52425 Jülich, Germany

E-mail: paruev@inr.ru

Received 19 January 2015, revised 3 April 2015

Accepted for publication 14 April 2015

Published 1 June 2015



CrossMark

Abstract

We study the non-resonant (non- ϕ) production of K^+K^- pairs by protons of 2.83 GeV kinetic energy on C, Cu, Ag and Au targets within the collision model, based on the nuclear spectral function, for incoherent primary proton–nucleon and secondary pion–nucleon creation processes. The model takes into account the initial proton and final kaon absorption, target nucleon binding and Fermi motion as well as nuclear mean-field potential effects on these processes. We calculate the antikaon momentum dependences of the exclusive absolute and relative K^+K^- pair yields in the acceptance window of the ANKE magnetic spectrometer, used in a recent experiment performed at COoler SYnchrotron (COSY), within the different scenarios for the antikaon–nucleus optical potential. We demonstrate that the above observables are strongly sensitive to this potential. Therefore, they can be useful to help determine the K^- optical potential from the direct comparison of the results of our calculations with the data from the respective ANKE-at-COSY experiment. We also show that the pion–nucleon production channels dominate in the low-momentum K^- , K^+ production in the considered kinematics and, hence, they have to be accounted for in the analysis of these data.

Keywords: kaon production, kaon in-medium potential, in-medium effects

(Some figures may appear in colour only in the online journal)

1. Introduction

The study of kaon and antikaon properties in a strongly interacting environment has been a very active research field over the last two decades (see, for example, [1–3]), especially in connection with the questions of the partial restoration of chiral symmetry in hot/dense nuclear matter and of the existence of the K^- condensate in neutron stars. From the analysis of KaoS [4], FOPI [5] and ANKE [6] data on K^+ production in heavy-ion and proton–nucleus reactions in the framework of transport approaches, [7] and [8] established that the K^+ meson ($K^+ = \bar{s}u$) feels a moderately repulsive nuclear potential of about 20–30 MeV at normal nuclear matter density ρ_0 , in agreement with theoretical calculations [3, 9]. A very recent result on the azimuthal emission pattern of K^+ mesons in Ni+Ni collisions at a beam kinetic energy of 1.91 A GeV, obtained by the FOPI Collaboration, also supports the existence of a repulsive kaon–nucleus potential of the same order of magnitude as that mentioned above [10]. Similar to K^+ , the K^0 meson in-medium nuclear potential is expected to be repulsive as well due to its quark content ($K^0 = \bar{s}d$). Indeed, the comparison of the ratio of the K^0 momentum distributions from π^- +Pb and π^- + C reactions at a pion incident momentum of 1.15 GeV/c, measured by the FOPI Collaboration, with hadron-string dynamics (HSD) transport model calculations, suggests a repulsive K^0 -nucleus optical potential of about 20 MeV at normal nuclear matter density [11]. Whereas the data on K^0 transverse momentum spectra in Ar+KCl and p +Nb reactions at bombarding kinetic energies of 1.756 A GeV and 3.5 GeV, collected recently by the HADES Collaboration, point to the existence of a stronger repulsive in-medium K^0 potential of about 35–40 MeV strength at saturation density ρ_0 for kaons at rest [12].

Contrary to the K^+ , K^0 mesons, the K^- meson ($K^- = s\bar{u}$) properties in nuclear matter are much less known nowadays and are still very intense debated. This is due to the fact that the antikaon can easily form baryonic resonances in the nuclear medium, which leads to the modification of its in-medium properties and requires complicated self-consistent coupled-channel calculations of this modification including the complete set of the pseudoscalar meson and baryon octets. Such calculations, based on a chiral Lagrangians [13–19] or on meson-exchange potentials [20, 21], predict a relatively shallow low-energy K^- -nucleus potential with a central depth of the order of -50 to -80 MeV. On the other hand, fits of the K^- atomic data [22] by the phenomenological density-dependent optical potentials as well as by these potentials and the relativistic mean-field calculations [23] lead to a deep potential of depth of about -200 MeV at density ρ_0 for antikaon in matter, which is in conflict with the results of the self-consistent approaches mentioned above. Recently, a chirally motivated meson–baryon coupled-channel model [24], which accounts for the subthreshold in-medium K^-N s -wave scattering amplitudes, produced K^- potential depths in the range of $-(80\text{--}90)$ MeV in kaonic atoms at nuclear matter density. However, by adding a ρ^2 -dependent phenomenological term, which could represent $\bar{K}NN \rightarrow YN$ absorption and dispersion, to improve the agreement with data, the antikaon potential becomes twice as deep [24, 25]. However, it should be noted that the antikaonic-atom data probe medium is at the surface of the nucleus and, therefore, does not provide the strong constraints on the K^- -nucleus potential at the normal nuclear matter density. The present status of the study of low-energy in-medium K^- nuclear interactions is given in [25].

Motivated by the fact that a very strong antikaon–nucleon potential could form deeply bound kaonic states [26], the experiments of KEK [27] and FINUDA [28] were performed to search for such states and, as a result, they claim evidence for their existence. In the DISTO experiment [29], an indication of a deeply bound compact K^-pp cluster formed in the

$pp \rightarrow p\Lambda K^+$ reaction at 2.85 GeV was obtained. An analysis of the final state of this reaction at a beam kinetic energy of 3.5 GeV with the aim of studying of the possible formation of an intermediate K^-pp bound-state in it has been carried out by the HADES Collaboration as well [30]. It was found that the data, which were collected with the HADES spectrometer, are compatible with the background-only hypothesis that includes no production of an intermediate kaonic cluster. Also, the more precise KEK experiment [31] did not observe a narrow structure in the proton spectrum following K^- absorption at rest in ^4He , which has been identified in [27] with a deeply bound K^-ppn cluster. In a recent J-PARC experiment [32], devoted to searching for the K^-pp bound state in the in-flight $^3\text{He}(K^-, n)$ reaction at 1 GeV/c, no significant peak was also observed in the neutron missing-mass spectrum in the region corresponding to K^-pp binding energy larger than 80 MeV, where a bump structure was reported in the Λp final state by the FINUDA and DISTO Collaborations. On the other hand, another very recent J-PARC experiment [33] claims evidence for the observation of a ‘ K^-pp ’-like structure in the $d(\pi^+, K^+)$ reaction at 1.69 GeV/c with binding energy of 95_{-17}^{+18} (stat.) $_{-21}^{+30}$ (syst.) MeV. Theoretically, it has been argued [34] that at present there is no experimental evidence both for the existence of deeply bound kaonic states and for a strong antikaon–nucleus potential with a central depth of the order of -200 MeV, claimed in the experiment [35].

Information about in-medium properties of antikaons can also be deduced from the study of their production both in heavy-ion and proton–nucleus collisions at incident energies near or below the free nucleon–nucleon threshold (2.5 GeV) because the dropping K^- mass scenario will lead to an enhancement of the K^- yield in these collisions due to in-medium shifts of the elementary production thresholds to lower energies. Thus, in particular, in [1, 3, 10] it was shown that the existence of a K^- condensate is not compatible with the available heavy-ion data. Analysis of the KaoS data on the ratio of K^- and K^+ inclusive momentum spectra from reactions $p + A \rightarrow K^\pm + X$ with $A = \text{C}$ and Au at laboratory angles from 36° to 60° and beam energy of 2.5 GeV within the BUU transport model has shown that these data are consistent with the in-medium K^-A potential of the order of -80 MeV at normal nuclear density [36]. A reasonable description of that measured at the ITEP accelerator, both including antikaon momentum distributions in the momentum range from 0.6 to 1.3 GeV/c at a laboratory angle of 10.5° in $p\text{Be}$, $p\text{Cu}$ interactions at 2.25, 2.4 GeV beam energies and K^- excitation functions in these interactions for K^- momentum of 1.28 GeV/c at bombarding energies < 3 GeV was, respectively, reached in [37] and in [38] in the frame of the folding model, based on the target nucleon momentum distribution and on free elementary cross sections, assuming vacuum K^+ , K^- masses. The K^- potential of ≈ -28 MeV at density ρ_0 and an antikaon momentum of 800 MeV/c was extracted in [39] from the data on elastic K^-A scattering within Glauber theory. So, one can conclude that the situation with the antikaon–nucleus optical potential is still very unclear.

To make progress in understanding the strength of the K^- interaction with a nuclear medium, it is necessary to carry out the exclusive measurements with the tagging the low-momentum K^- mesons not stemming from the vacuum ϕ decays and, therefore, leading to ‘genuine’ information about this strength. Such measurements have been recently performed by the ANKE Collaboration at COSY, which studied the production of K^+K^- pairs in proton collisions with C, Cu, Ag and Au targets at an incident beam energy of 2.83 GeV for the K^+K^- invariant masses belonging to the ϕ and non- ϕ regions [40, 41]. For the first time, in the ϕ region, the momentum dependence of the ϕ nuclear transparency ratio, the in-medium ϕ meson width and the differential cross section for its production at forward angles were determined for these targets over the ϕ momentum range of 0.6–1.6 GeV/c

[40, 41]. For the purpose of obtaining the exclusive differential cross section for K^+K^- pair production on the considered target nuclei as a function of the laboratory K^- momentum, further analysis of the data coming from the non- ϕ region of the K^+K^- invariant mass is currently being carried out.

In this respect, the main purpose of the present work is to estimate the absolute and relative yields of non-resonant (not through the vacuum $\phi \rightarrow K^+K^-$ decays⁴) K^+K^- pairs from pA collisions at a beam energy of 2.83 GeV in the acceptance window of the ANKE spectrometer used in the experiment [40, 41] performed at the COSY accelerator in the framework of the collision model, based on the nuclear spectral function, for incoherent primary proton–nucleon and secondary pion–nucleon K^+K^- creation processes in different scenarios for the K^- nuclear potential. In view of the expected data from this experiment, the estimates can be used as an important tool for determining the antikaon–nucleus optical potential.

2. The model

2.1. Direct non-resonant K^+K^- pair production mechanism

The direct non-resonant (non- ϕ) production of K^+K^- pairs in pA reactions at an initial energy of 2.83 GeV can occur due to the nucleon’s Fermi motion in the following elementary processes with zero, one and two pions in the final states⁵:

$$p + p \rightarrow K^+ + K^- + p + p, \quad (1)$$

$$p + p \rightarrow K^+ + K^- + N + N + m\pi; \quad (2)$$

$$p + n \rightarrow K^+ + K^- + p + n, \quad (3)$$

$$p + n \rightarrow K^+ + K^- + N + N + m\pi, \quad (4)$$

where $m = 1, 2$. In the following calculations, we will include the medium modification of the final nucleons, kaon and antikaon, participating in the production processes (1)–(4), by using the in-medium cross sections of these processes, for reasons of numerical simplicity, instead of their local effective masses $m_h^*(r)$ their average in-medium masses $\langle m_h^* \rangle$ defined in line with [43–45] as:

⁴ Since the ϕ mesons produced in pA reactions at an incident energy of 2.83 GeV have large momenta [41], most of them will decay outside the nucleus. Moreover, the total cross section of the reaction $pp \rightarrow pp\phi \rightarrow ppK^+K^-$, as is seen from figure 1, is more than one order of magnitude less than that of the non-resonant K^+K^- pair production in pp collisions at excess energies $\epsilon_{K\bar{K}}$ above the K^+K^-pp threshold $\sqrt{s_{\text{th}}}$, $\epsilon_{K\bar{K}} = \sqrt{s} - \sqrt{s_{\text{th}}}$ (\sqrt{s} is the total center-of-mass energy), falling in the range of 0.1–0.5 GeV, which mainly contribute, as our estimates showed, to the K^+K^- creation in the primary processes at this incident energy considered in the next section. Therefore, we can neglect the possible contribution of the distorted due to the FSI K^+K^- pairs stemming from the in-medium $\phi \rightarrow K^+K^-$ decays to the ‘genuine’ non-resonant kaon pair production.

⁵ It should be pointed out that the K^+K^- pairs can also be produced in the elementary reaction channel non- ϕ $pn \rightarrow dK^+K^-$ studied recently in the threshold energy region by the ANKE Collaboration [42]. However, its contribution to the kaon pair creation in pA collisions at beam energy of 2.83 GeV is expected [37] to be insignificant at the antikaon momenta < 0.9 GeV/ c of our current interest.

$$\langle m_h^* \rangle = m_h + U_h^0 \frac{\langle \rho_N \rangle}{\rho_0} + V_{\text{ch}}(R_{1/2}). \quad (5)$$

Here, m_h is the hadron free space mass⁶, U_h^0 is its nuclear potential depth at saturation density ρ_0 , $\langle \rho_N \rangle$ is the average nucleon density⁷ and $V_{\text{ch}}(R_{1/2})$ is the charged hadron Coulomb potential⁸ taken at the point $R_{1/2}$ at which the local nucleon density $\rho_N(r)$ satisfies the relation $\rho_N(R_{1/2}) = \rho_0/2$. In the subsequent study for the K^+ and K^- mass shifts $U_{K^+}^0$ and $U_{K^-}^0$, we will employ the following options: $U_{K^+}^0 = 22$ MeV [43] and (i) $U_{K^-}^0 = 0$, (ii) $U_{K^-}^0 = -60$ MeV, (iii) $U_{K^-}^0 = -126$ MeV [43], and (iv) $U_{K^-}^0 = -180$ MeV. One can see that the second option corresponds to the shallow antikaon–nucleus potential, whereas the third and fourth ones represent, respectively, the relatively deep and deep K^-A optical potentials. Accounting for that the relation between the effective scalar nucleon potential U_N^0 , entering into the equation (5), and the corresponding Schrödinger equivalent potential V_{NA}^{SEP} at the normal nuclear matter density is given by

$$U_N^0 = \frac{\sqrt{m_N^2 + p_N^2}}{m_N} V_{NA}^{\text{SEP}} \quad (6)$$

as well as the fact that the momenta p_N of the outgoing in reactions (1)–(4) nucleons are, as showed our calculations, around of momentum of 1 GeV/ c and using that $V_{NA}^{\text{SEP}} \approx 25$ MeV at this momentum [47], we can readily obtain that $U_N^0 \approx 35$ MeV. We will employ this potential throughout our present work. The total energy E'_h of the hadron inside the nuclear medium can be expressed through its average effective mass $\langle m_h^* \rangle$ defined above and its in-medium momentum \mathbf{p}'_h as in the free particle case, namely:

$$E'_h = \sqrt{(\langle m_h^* \rangle)^2 + (\mathbf{p}'_h)^2}. \quad (7)$$

The momentum \mathbf{p}'_h is related to the vacuum one \mathbf{p}_h by the following expression:

$$E'_h = \sqrt{(\langle m_h^* \rangle)^2 + (\mathbf{p}'_h)^2} = \sqrt{m_h^2 + \mathbf{p}_h^2} = E_h, \quad (8)$$

where E_h is the hadron vacuum total energy.

Then, taking into consideration the distortions of the initial proton and final kaons as well as the fact that in the ANKE experiment the latter were detected in the forward polar angle domain $0^\circ \leq \theta_{K^+,K^-} \leq 12^\circ$ and using the results given in [37, 43–45], we can represent the exclusive differential cross section for the production of K^+ meson with the vacuum momentum \mathbf{p}_{K^+} in coincidence with the K^- meson with the vacuum momentum \mathbf{p}_{K^-} off nuclei in the primary proton-induced reaction channels (1)–(4) as follows:

$$\frac{d\sigma_{pA \rightarrow K^+K^-X}^{(\text{prim})}(\mathbf{p}_0, \mathbf{p}_{K^+}, \mathbf{p}_{K^-})}{d\mathbf{p}_{K^+} d\mathbf{p}_{K^-}} = I_V [A] \quad (9)$$

⁶ The bare kaon and antikaon masses are denoted by m_K .

⁷ Which is assumed to be equal to $\rho_0/2$ [46] for all considered target nuclei.

⁸ It is worth mentioning that this potential for kaons and protons amounts approximately to 3.5, 9.7, 12.3, and 16.6 MeV for C, Cu, Ag and Au nuclei, respectively [44], i.e. for heavy nuclei like Au it is of the same order of magnitude as the repulsive K^+ nuclear mean-field potential.

$$\begin{aligned} & \times \left[\frac{Z}{A} \left\langle \frac{d\sigma_{pp \rightarrow K^+K^-X}^{\text{nr}}(\mathbf{p}'_0, \mathbf{p}'_{K^+}, \mathbf{p}'_{K^-})}{d\mathbf{p}'_{K^+} d\mathbf{p}'_{K^-}} \right\rangle_A \right. \\ & \left. + \frac{N}{A} \left\langle \frac{d\sigma_{pn \rightarrow K^+K^-X}^{\text{nr}}(\mathbf{p}'_0, \mathbf{p}'_{K^+}, \mathbf{p}'_{K^-})}{d\mathbf{p}'_{K^+} d\mathbf{p}'_{K^-}} \right\rangle_A \right] \frac{d\mathbf{p}'_{K^+} d\mathbf{p}'_{K^-}}{d\mathbf{p}_{K^+} d\mathbf{p}_{K^-}}, \end{aligned}$$

where

$$I_V[A] = 2\pi A \int_0^R r_\perp dr_\perp \int_{-\sqrt{R^2-r_\perp^2}}^{\sqrt{R^2-r_\perp^2}} dz \rho(\sqrt{r_\perp^2 + z^2}) \quad (10)$$

$$\begin{aligned} & \times \exp \left[-\sigma_{pN}^{\text{in}} A \int_{-\sqrt{R^2-r_\perp^2}}^z \rho(\sqrt{r_\perp^2 + x^2}) dx - \sigma_{K^+N}^{\text{tot}} A \int_z^{\sqrt{R^2-r_\perp^2}} \rho(\sqrt{r_\perp^2 + x^2}) dx \right] \\ & \times \exp \left[-\int_z^{\sqrt{R^2-r_\perp^2}} \mu_{K^-N} [p'_{K^-}(\sqrt{r_\perp^2 + x^2})] \rho(\sqrt{r_\perp^2 + x^2}) dx \right], \\ & \left\langle \frac{d\sigma_{pN \rightarrow K^+K^-X}^{\text{nr}}(\mathbf{p}'_0, \mathbf{p}'_{K^+}, \mathbf{p}'_{K^-})}{d\mathbf{p}'_{K^+} d\mathbf{p}'_{K^-}} \right\rangle_A = \iint P_A(\mathbf{p}_t, E) d\mathbf{p}_t dE \quad (11) \\ & \times \left\{ \frac{d\sigma_{pN \rightarrow K^+K^-X}^{\text{nr}}[\sqrt{s}, \langle m_{K^+}^* \rangle, \langle m_{K^-}^* \rangle, \langle m_N^* \rangle, \langle m_N^* \rangle, \mathbf{p}'_{K^+}, \mathbf{p}'_{K^-}]}{d\mathbf{p}'_{K^+} d\mathbf{p}'_{K^-}} \right\} \end{aligned}$$

and

$$\mu_{K^-N}[p'_{K^-}(r')] = \sigma_{K^-p}^{\text{tot}}[p'_{K^-}(r')]Z + \sigma_{K^-n}^{\text{tot}}[p'_{K^-}(r')]N, \quad (12)$$

$$p'_{K^-}(r') = \sqrt{E_{K^-}^2 - [m_{K^-}^*(r')]^2}, \quad (13)$$

$$m_{K^-}^*(r') = m_K + U_{K^-}^0 \frac{\rho_N(r')}{\rho_0} + V_{cK^-}(r'), \quad (14)$$

$$r' = \sqrt{r_\perp^2 + x^2}. \quad (15)$$

Here, $d\sigma_{pN \rightarrow K^+K^-X}^{\text{nr}}[\sqrt{s}, \langle m_{K^+}^* \rangle, \langle m_{K^-}^* \rangle, \langle m_N^* \rangle, \langle m_N^* \rangle, \mathbf{p}'_{K^+}, \mathbf{p}'_{K^-}]/d\mathbf{p}'_{K^+} d\mathbf{p}'_{K^-}$ are the ‘in-medium’ differential cross sections for the non-resonant production of K^+ and K^- mesons with the in-medium momenta \mathbf{p}'_{K^+} and \mathbf{p}'_{K^-} , respectively, in reactions (1) and (2) ($N=p$) as well as

in (3) and (4) ($N = n$) at the pN center-of-mass energy \sqrt{s} ⁹; $\rho(r)$ and $P_A(\mathbf{p}_t, E)$ are the local nucleon density and the spectral function of target nucleus A normalized to unity¹⁰; \mathbf{p}_t and E are the internal momentum and binding energy of the struck target nucleon just before the collision; σ_{pN}^{in} and $\sigma_{K^+N}^{\text{tot}}, \sigma_{K^-N}^{\text{tot}}$ are the inelastic and total cross sections of the free pN and K^+N , K^-N interactions¹¹; Z and N are the numbers of protons and neutrons in the target nucleus ($A = Z + N$), R is its radius; \mathbf{p}_0 and \mathbf{p}'_0 are the momenta of the initial proton outside and inside the target nucleus¹². The quantity $I_V[A]$ in equation (9) represents the effective number of target nucleons participating in the primary $pN \rightarrow K^+K^-X$ reactions. It is determined, in particular, by the one nucleon K^- absorption and does not account for the two nucleon antikaon absorption mechanism discussed in [46]. The inclusion of the K^- absorption by pairs of nucleons of 20% that of the one body absorption in line with [46] leads to only small corrections to the quantity $I_V[A]$ ¹³. They are within 1%–3% for the gold nucleus and for the antikaon momenta of interest, as our calculations for this nucleus with the diffuse boundary showed. Therefore, we ignored the two nucleon K^- absorption mechanism in the present study.

In our calculations of the non-resonant K^+K^- pair creation in pA interactions reported below, the in-medium exclusive differential cross sections $d\sigma_{pN \rightarrow K^+K^-X}^{\text{nr}}[\sqrt{s}, \langle m_{K^+}^* \rangle, \langle m_{K^-}^* \rangle, \langle m_N^* \rangle, \langle m_N^* \rangle, \mathbf{p}'_{K^+}, \mathbf{p}'_{K^-}]/d\mathbf{p}'_{K^+}d\mathbf{p}'_{K^-}$ have been described according to the four-body phase space (see, also, [43])¹⁴:

$$\begin{aligned} & \frac{d\sigma_{pN \rightarrow K^+K^-X}^{\text{nr}}[\sqrt{s}, \langle m_{K^+}^* \rangle, \langle m_{K^-}^* \rangle, \langle m_N^* \rangle, \langle m_N^* \rangle, \mathbf{p}'_{K^+}, \mathbf{p}'_{K^-}]}{d\mathbf{p}'_{K^+}d\mathbf{p}'_{K^-}} \\ &= \frac{\sigma_{pN \rightarrow K^+K^-X}^{\text{nr}}(\sqrt{s}, \sqrt{s_{\text{th}}^*})}{4E'_{K^+}E'_{K^-}} \\ & \times \frac{I_2(s_2, \langle m_N^* \rangle, \langle m_N^* \rangle)}{I_4(s, \langle m_{K^+}^* \rangle, \langle m_{K^-}^* \rangle, \langle m_N^* \rangle, \langle m_N^* \rangle)}, \end{aligned} \quad (16)$$

⁹ The expression for s is given in [43] by the formula (18).

¹⁰ The specific information about the quantities used in our subsequent calculations is given in [43–45, 48].

¹¹ We use $\sigma_{pN}^{\text{in}} = 30$ mb for the considered projectile proton energy and $\sigma_{K^+N}^{\text{tot}} = 12$ mb for all kaon momenta of interest [37] in our calculations. For the antikaon-nucleon total cross sections $\sigma_{K^-p}^{\text{tot}}(p_{K^-})$, $\sigma_{K^-n}^{\text{tot}}(p_{K^-})$ as functions of the K^- momentum p_{K^-} we employ in them the corresponding parametrizations suggested in [49] (see, also, [37]). Dealing with the total cross sections $\sigma_{K^{\pm}N}^{\text{tot}}$ in (10), we assume that if a kaon undergoes a quasi-elastic collision with the intranuclear nucleon it will not fall in the ANKE acceptance window.

¹² They are linked by the equation (13) from [43].

¹³ And to the quantity $I_V^{\text{sec}}[A]$, determining the differential cross section for non-resonant K^+K^- pair production in pA reactions from the two-step creation mechanism (see below), as our calculations also showed.

¹⁴ It should be noted that this space was found [50–52] to be distorted mostly by the pp and K^-p FSI in the non-resonant $pp \rightarrow ppK^+K^-$ reaction both at a beam energy of 2.83 GeV and at incident energies below the ϕ meson production threshold. However, since we are interested in the exclusive cross sections for K^+K^- production in pA reactions averaged over the ANKE acceptance polar angle domain $0^\circ \leq \theta_{K^+,K^-} \leq 12^\circ$ (see below), but not in the full differential ones, one may hope that the account of this distortion as well as the deviation of the differential cross sections for the K^+K^-NN production in reactions (2) and (4) from those dictated by the four-body phase space leads to insignificant corrections.

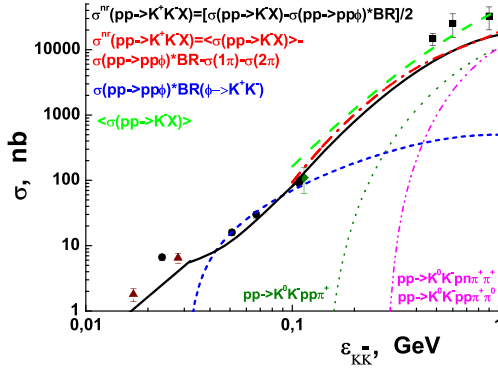


Figure 1. The kaon and kaon–antikaon production total cross sections in proton–proton collisions as functions of the excess energy above the K^+K^-pp threshold. For notation see the text.

where

$$I_2(s_2, \langle m_N^* \rangle, \langle m_N^* \rangle) = \left(\frac{\pi}{2} \right) \frac{\lambda \left[s_2, \left(\langle m_N^* \rangle \right)^2, \left(\langle m_N^* \rangle \right)^2 \right]}{s_2}, \quad (17)$$

$$s_2 = s + s'_{K^+K^-} - 2(E'_0 + E_t)(E'_{K^+} + E'_{K^-}) + 2(\mathbf{p}'_0 + \mathbf{p}_t)(\mathbf{p}'_{K^+} + \mathbf{p}'_{K^-}), \quad (18)$$

$$s'_{K^+K^-} = (E'_{K^+} + E'_{K^-})^2 - (\mathbf{p}'_{K^+} + \mathbf{p}'_{K^-})^2 \quad (19)$$

and the quantities E'_0 , E_t , I_4 and λ are defined in [43] by the equations (12), (15) (28) and (29), respectively. Here, $\sigma_{pN \rightarrow K^+K^-X}(\sqrt{s}, \sqrt{s_{th}^*})$ are the ‘in-medium’ total cross sections for the non-resonant K^+K^- pair production in reactions (1) and (2) ($N = p$) as well as in (3) and (4) ($N = n$) having the threshold energy $\sqrt{s_{th}^*} = \langle m_{K^+}^* \rangle + \langle m_{K^-}^* \rangle + 2 \langle m_N^* \rangle$. Following [43], we assume that these cross sections are equivalent to the vacuum ones $\sigma_{pN \rightarrow K^+K^-X}(\sqrt{s}, \sqrt{s_{th}})$ in which the free threshold energy $\sqrt{s_{th}} = 2(m_K + m_N)$ is replaced by the in-medium threshold one $\sqrt{s_{th}^*}$.

Let us now specify the total cross sections $\sigma_{pp \rightarrow K^+K^-X}(\sqrt{s}, \sqrt{s_{th}})$ and $\sigma_{pn \rightarrow K^+K^-X}(\sqrt{s}, \sqrt{s_{th}})$. Due to the lack of experimental information about the non-resonant production of K^+K^- pairs in pp interactions (1) and (2) at excess energies above the π meson mass m_π , the first cross section can be defined as:

$$\sigma_{pp \rightarrow K^+K^-X}(\sqrt{s}, \sqrt{s_{th}}) = \sigma_{pp \rightarrow K^-X}(\sqrt{s}, \sqrt{s_{th}}) - \sigma_{pp \rightarrow pp\phi}(\sqrt{s})BR(\phi \rightarrow K^+K^-) \quad (20)$$

$$- \sigma_{pp \rightarrow K^0 K^- pp\pi^+}(\sqrt{s}) - \sigma_{pp \rightarrow K^0 K^- pn\pi^+\pi^+}(\sqrt{s}) - \sigma_{pp \rightarrow K^0 K^- pp\pi^0\pi^+}(\sqrt{s}),$$

where $\sigma_{pp \rightarrow K^-X}(\sqrt{s}, \sqrt{s_{th}})$, $\sigma_{pp \rightarrow pp\phi}(\sqrt{s})$, $\sigma_{pp \rightarrow K^0 K^- pp\pi^+}(\sqrt{s})$, $\sigma_{pp \rightarrow K^0 K^- pn\pi^+\pi^+}(\sqrt{s})$ and $\sigma_{pp \rightarrow K^0 K^- pp\pi^0\pi^+}(\sqrt{s})$ are the total cross sections of the reactions $pp \rightarrow K^-X$, $pp \rightarrow pp\phi$, $pp \rightarrow K^0 K^- pp\pi^+$, $pp \rightarrow K^0 K^- pn\pi^+\pi^+$ and $pp \rightarrow K^0 K^- pp\pi^0\pi^+$, respectively, whereas

$BR(\phi \rightarrow K^+K^-) = 0.491$ ¹⁵. The available experimental data for the three latter channels are quite scarce and they were approximated in [53] by formulas (63), (64) and (67), which we adopt for our present study. The results of calculations of the total cross section of the first channel and the sum of the total cross sections of the second and third ones, according to them, are shown in figure 1 by dotted and dashed–dotted–dotted lines, respectively. For the total cross section $\sigma_{pp \rightarrow pp\phi}(\sqrt{s})$ we have used in it parametrization (12) from [48], which was multiplied by the factor of 0.75 in the light of the improved data on the ϕ production total cross section obtained in [50, 51]. Multiplying this cross section on the branching ratio of the ϕ decay into K^+K^- pair, we get the total cross section of the reaction $pp \rightarrow pp\phi \rightarrow ppK^+K^-$, which is shown in figure 1 by a short-dashed line. Up to now, there have been no data on the inclusive cross section $\sigma_{pp \rightarrow K^-X}(\sqrt{s}, \sqrt{s_{\text{th}}})$ at excess energies $m_\pi < \epsilon_{KR} < 0.5$ GeV of our interest and the existing parametrizations (31) from [43] and (4) from [54] provide different predictions for this cross section (see figure 1 in [43])¹⁶. Due to this fact, to reduce the uncertainty in determination of the cross section (20) it is natural to estimate it by using both of these parametrizations and for this cross section to take an arithmetic average of the obtained results. Such a procedure has been carried out and after it was found that the above average, presented in figure 1 by dotted–dashed curve, can be well fitted by the following expression:

$$\sigma_{pp \rightarrow K^+K^-X}^{\text{nr}}(\sqrt{s}, \sqrt{s_{\text{th}}}) = \frac{1}{2} \left[\sigma_{pp \rightarrow K^-X}(\sqrt{s}, \sqrt{s_{\text{th}}}) - \sigma_{pp \rightarrow pp\phi}(\sqrt{s}) BR(\phi \rightarrow K^+K^-) \right], \quad (21)$$

where inclusive cross section $\sigma_{pp \rightarrow K^-X}(\sqrt{s}, \sqrt{s_{\text{th}}})$ is taken from [43] in parametrization (31) (solid line in figure 1). As can be seen from figure 1, this expression also reproduces reasonably well the available experimental data on the non- ϕ contribution to the $pp \rightarrow K^+K^-pp$ total cross section at low excess energies from DISTO [55] (full diamond), COSY-11 [56] (full triangles) and ANKE [50–52] (full circles) Collaborations. Since there are no data for K^+K^- production in pn reactions (3), (4), to determine their cross sections—which provide a major source of uncertainty in our consideration—one needs to employ some models. In the present study, to estimate the ratio of the free total cross sections for K^+K^- production in pn and pp interactions, we have adopted the one-pion-exchange model [57, 58]. It gives [58] for the ratio of the total cross sections of the reactions $pp \rightarrow K^+\bar{K}^0pn$ and $pp \rightarrow K^0\bar{K}^0pp$ factor of 4, which is well in line with the available experimental data. Evidently, this enables us to use the above model to estimate the ratio between the free total cross sections of reactions (3) and (1) as well as to expect the obtained ratio to be essentially correct and meaningful. Employing the ratios (8) between total cross sections of different charge channels $\pi N \rightarrow K\bar{K}N$ found in [58] and accounting for that within the one-pion-exchange model the reaction (1) is described by the four diagrams with the exchanged π^0 meson and the process (3) also represented by the four diagrams, respectively, with the exchanged π^0, π^0, π^+ and π^- mesons, we get the value of 4.5 for this ratio¹⁷. Since detailed information about the reactions $\pi N \rightarrow K\bar{K}N\pi$ is not available, we shall not concern ourselves here with this type of model to estimate the ratio of the total cross sections of channels (4) and (2) and will assume that in the relevant energy region the cross section

¹⁵ We neglect the possible modification of the branching ratio of the decay $\phi \rightarrow K^+K^-$ in the nuclear medium.

¹⁶ Their arithmetic average is depicted in figure 1 by a long-dashed curve, which is well in line with the inclusive $pp \rightarrow K^-X$ data (full squares) at higher energies taken from [43].

¹⁷ In this connection it should be noted that the ratio of the free total cross sections of the reactions $pn \rightarrow pn\phi \rightarrow pnK^+K^-$ and $pp \rightarrow pp\phi \rightarrow ppK^+K^-$ is about 3–5 as follows from the results obtained in [59] within an effective meson–nucleon theory.

$\sigma_{pn \rightarrow K^+K^-X}^{\text{nr}}(\sqrt{s}, \sqrt{s_{\text{th}}})$ is related to $\sigma_{pp \rightarrow K^+K^-X}^{\text{nr}}(\sqrt{s}, \sqrt{s_{\text{th}}})$, defined above by equation (21), as:

$$\sigma_{pn \rightarrow K^+K^-X}^{\text{nr}}(\sqrt{s}, \sqrt{s_{\text{th}}}) = 4.5 \sigma_{pp \rightarrow K^+K^-X}^{\text{nr}}(\sqrt{s}, \sqrt{s_{\text{th}}}). \quad (22)$$

The primary elementary cross sections (21) and (22) will be used below to calculate the yield of K^+K^- pairs from proton–nucleus collisions.

Let us now define the exclusive differential cross section for the non-resonant K^+K^- production in pA collisions from primary processes (1)–(4), corresponding to the kinematical conditions of the ANKE experiment. In this experiment, the differential cross section for production of K^- mesons in the polar angular range of $0^\circ \leq \theta_{K^-} \leq 12^\circ$ in a laboratory system in the interaction of protons of energy of 2.83 GeV with the C, Cu, Ag and Au target nuclei in coincidence with K^+ mesons, which were required to have vacuum momenta in the interval of $0.2 \text{ GeV}/c \leq p_{K^+} \leq 0.6 \text{ GeV}/c$ and to be in the same polar angular domain in l.s. as that for antikaons— $0^\circ \leq \theta_{K^+} \leq 12^\circ$, was measured as a function of their vacuum momentum. Additionally, the invariant mass of the detected K^+K^- pair, $IM(K^+K^-)$, was required to be less than 1.005 GeV. Keeping this in mind and imposing the respective integrations on the full exclusive differential cross section (9), we can represent this differential cross section in the following form:

$$\begin{aligned} \frac{d\sigma_{pA \rightarrow K^+K^-X}^{\text{(prim)}}(\mathbf{p}_0, AW, p_{K^-})}{dp_{K^+} d\Omega_{K^+} dp_{K^-} d\Omega_{K^-}} &= \frac{1}{(2\pi)^2 (1 - \cos 12^\circ)^2} \frac{1}{0.4 \text{ GeV}/c} \quad (23) \\ &\times \int_{0.2 \text{ GeV}/c}^{0.6 \text{ GeV}/c} dp_{K^+} \int_{\cos 12^\circ}^1 d\cos\theta_{K^+} \int_{\cos 12^\circ}^1 d\cos\theta_{K^-} \int_0^{2\pi} d\phi_{K^+} \int_0^{2\pi} d\phi_{K^-} \\ &\times \frac{d\sigma_{pA \rightarrow K^+K^-X}^{\text{(prim)}}(\mathbf{p}_0, \mathbf{p}_{K^+}, \mathbf{p}_{K^-})}{d\mathbf{p}_{K^+} d\mathbf{p}_{K^-}} p_{K^+}^2 p_{K^-}^2 \theta[1.005 \text{ GeV} - IM(K^+K^-)], \end{aligned}$$

where

$$AW = 0.2 \text{ GeV}/c \leq p_{K^+} \leq 0.6 \text{ GeV}/c, \quad 0^\circ \leq \theta_{K^\pm} \leq 12^\circ, \quad IM(K^+K^-) \leq 1.005 \text{ GeV}; \quad (24)$$

$$IM(K^+K^-) = \sqrt{(E_{K^+} + E_{K^-})^2 - (\mathbf{p}_{K^+} + \mathbf{p}_{K^-})^2}. \quad (25)$$

Here, ϕ_{K^+} and ϕ_{K^-} are the azimuthal angles of kaon and antikaon momenta \mathbf{p}_{K^+} and \mathbf{p}_{K^-} in the laboratory system and $\theta(x)$ is the standard step function.

2.2. Two-step non-resonant K^+K^- pair production mechanism

At the initial energy of our interest, 2.83 GeV, the following two-step processes with pions in intermediate states may contribute to the non-resonant kaon pair production in pA reactions:

$$p + N_1 \rightarrow \pi + X, \quad (26)$$

$$\pi + N_2 \rightarrow N + K^+ + K^-. \quad (27)$$

Here, N_1, N_2, N and π stand for p, n and π^+, π^0, π^- for the specific isospin channel. Using the results given in [37, 43, 48] and accounting for equation (9), the exclusive differential non-resonant K^+K^- production cross section for pA collisions at small laboratory angles from the secondary channels (27) can be represented as follows:

$$\begin{aligned}
\frac{d\sigma_{\rho A \rightarrow K^+ K^- X}^{(\text{sec})}(\mathbf{p}_0, \mathbf{p}_{K^+}, \mathbf{p}_{K^-})}{d\mathbf{p}_{K^+} d\mathbf{p}_{K^-}} &= \frac{I_V^{\text{sec}}[A]}{I_V[A]} \sum_{\pi'=\pi^+, \pi^0, \pi^-} \int_{4\pi} d\Omega_\pi \int_{p_\pi^{\text{abs}}}^{p_\pi^{\text{lim}}(\theta_\pi)} p_\pi^2 dp_\pi \frac{d\sigma_{\rho A \rightarrow \pi' X}^{(\text{prim})}(\mathbf{p}_0)}{d\mathbf{p}_\pi} \\
&\times \left[\frac{Z}{A} \left\langle \frac{d\sigma_{\pi' p \rightarrow NK^+ K^-}^{\text{nr}}(\mathbf{p}_\pi, \mathbf{p}'_{K^+}, \mathbf{p}'_{K^-})}{d\mathbf{p}'_{K^+} d\mathbf{p}'_{K^-}} \right\rangle_A \right. \\
&\quad \left. + \frac{N}{A} \left\langle \frac{d\sigma_{\pi' n \rightarrow NK^+ K^-}^{\text{nr}}(\mathbf{p}_\pi, \mathbf{p}'_{K^+}, \mathbf{p}'_{K^-})}{d\mathbf{p}'_{K^+} d\mathbf{p}'_{K^-}} \right\rangle_A \right] \frac{d\mathbf{p}'_{K^+} d\mathbf{p}'_{K^-}}{d\mathbf{p}_{K^+} d\mathbf{p}_{K^-}},
\end{aligned} \tag{28}$$

where

$$\begin{aligned}
I_V^{\text{sec}}[A] &= 2\pi A^2 \int_0^R r_\perp dr_\perp \int_{-\sqrt{R^2-r_\perp^2}}^{\sqrt{R^2-r_\perp^2}} dz \rho(\sqrt{r_\perp^2+z^2}) \int_0^{\sqrt{R^2-r_\perp^2}-z} dl \rho(\sqrt{r_\perp^2+(z+l)^2}) \\
&\times \exp \left[-\sigma_{\rho N}^{\text{in}} A \int_{-\sqrt{R^2-r_\perp^2}}^z \rho(\sqrt{r_\perp^2+x^2}) dx - \sigma_{\pi N}^{\text{tot}} A \int_z^{z+l} \rho(\sqrt{r_\perp^2+x^2}) dx \right] \\
&\times \exp \left[-\sigma_{K^+ N}^{\text{tot}} A \int_{z+l}^{\sqrt{R^2-r_\perp^2}} \rho(\sqrt{r_\perp^2+x^2}) dx \right. \\
&\quad \left. - \int_{z+l}^{\sqrt{R^2-r_\perp^2}} \mu_{K^- N} \left[p'_{K^-}(\sqrt{r_\perp^2+x^2}) \right] \rho(\sqrt{r_\perp^2+x^2}) dx \right]
\end{aligned} \tag{29}$$

and

$$\begin{aligned}
\left\langle \frac{d\sigma_{\pi' N \rightarrow NK^+ K^-}^{\text{nr}}(\mathbf{p}_\pi, \mathbf{p}'_{K^+}, \mathbf{p}'_{K^-})}{d\mathbf{p}'_{K^+} d\mathbf{p}'_{K^-}} \right\rangle_A &= \iint P_A(\mathbf{p}_i, E) d\mathbf{p}_i dE \\
&\times \left\{ \frac{d\sigma_{\pi' N \rightarrow NK^+ K^-}^{\text{nr}}[\sqrt{s_1}, \langle m_{K^+}^* \rangle, \langle m_{K^-}^* \rangle, \langle m_N^* \rangle, \mathbf{p}'_{K^+}, \mathbf{p}'_{K^-}]}{d\mathbf{p}'_{K^+} d\mathbf{p}'_{K^-}} \right\}.
\end{aligned} \tag{30}$$

Here, $d\sigma_{\pi' N \rightarrow NK^+ K^-}^{\text{nr}}[\sqrt{s_1}, \langle m_{K^+}^* \rangle, \langle m_{K^-}^* \rangle, \langle m_N^* \rangle, \mathbf{p}'_{K^+}, \mathbf{p}'_{K^-}]/d\mathbf{p}'_{K^+} d\mathbf{p}'_{K^-}$ are the ‘in-medium’ exclusive differential cross sections for the non-resonant production of K^+ and K^- mesons with the in-medium momenta \mathbf{p}'_{K^+} and \mathbf{p}'_{K^-} , respectively, in reactions (27) at the πN centre-of-mass energy $\sqrt{s_1}$ and the other quantities, entering into equations (28) and (29), are defined in [37, 43, 48].

The elementary $K^+ K^-$ creation processes $\pi^+ n \rightarrow p K^+ K^-$, $\pi^0 p \rightarrow p K^+ K^-$, $\pi^0 n \rightarrow n K^+ K^-$ and $\pi^- p \rightarrow n K^+ K^-$ have been included in our calculations of the non-resonant kaon pair production on nuclei. In them, the exclusive differential cross sections $d\sigma_{\pi' N \rightarrow NK^+ K^-}^{\text{nr}}[\sqrt{s_1}, \langle m_{K^+}^* \rangle, \langle m_{K^-}^* \rangle, \langle m_N^* \rangle, \mathbf{p}'_{K^+}, \mathbf{p}'_{K^-}]/d\mathbf{p}'_{K^+} d\mathbf{p}'_{K^-}$ have been computed according to the three-body phase space [43] accounting for the medium effects on the outgoing in reactions (27) nucleons, kaons and antikaons on the same footing as that employed in calculating the $K^+ K^-$ production cross sections (16) from primary proton-

induced reaction channels:

$$\begin{aligned}
& \frac{d\sigma_{\pi'N \rightarrow NK^+K^-}^{\text{nr}} \left[\sqrt{s_1}, \langle m_{K^+}^* \rangle, \langle m_{K^-}^* \rangle, \langle m_N^* \rangle, \mathbf{p}'_{K^+}, \mathbf{p}'_{K^-} \right]}{d\mathbf{p}'_{K^+} d\mathbf{p}'_{K^-}} \\
&= \frac{\sigma_{\pi'N \rightarrow NK^+K^-}^{\text{nr}} \left(\sqrt{s_1}, \sqrt{s_{1,\text{th}}^*} \right)}{8E'_{K^+} E'_{K^-}} \\
&\times \frac{1}{I_3 \left(s_1, \langle m_{K^+}^* \rangle, \langle m_{K^-}^* \rangle, \langle m_N^* \rangle \right)} \\
&\times \frac{1}{(\omega_1 + E_t)} \delta \left[\omega_1 + E_t - \sqrt{\left(\langle m_N^* \rangle \right)^2 + \left(\mathbf{Q}_1 + \mathbf{p}_t \right)^2} \right],
\end{aligned} \tag{31}$$

where

$$\omega_1 = E_\pi - E'_{K^+} - E'_{K^-}, \quad \mathbf{Q}_1 = \mathbf{p}_\pi - \mathbf{p}'_{K^+} - \mathbf{p}'_{K^-}, \tag{32}$$

\mathbf{p}_π and E_π are the momentum and total energy of an intermediate pion (which is assumed to be on-shell), I_3 is the three-body phase space defined in [43] by the formula (27). In equation (31), $\sigma_{\pi'N \rightarrow NK^+K^-}^{\text{nr}}(\sqrt{s_1}, \sqrt{s_{1,\text{th}}^*})$ are the ‘in-medium’ total cross sections for the non-resonant K^+K^- pair production in reactions (27) having the threshold energy $\sqrt{s_{1,\text{th}}^*} = \langle m_{K^+}^* \rangle + \langle m_{K^-}^* \rangle + \langle m_N^* \rangle$. As before, we assume that these cross sections are equivalent to the vacuum ones $\sigma_{\pi'N \rightarrow NK^+K^-}^{\text{nr}}(\sqrt{s_1}, \sqrt{s_{1,\text{th}}})$ in which the free threshold energy $\sqrt{s_{1,\text{th}}} = 2m_K + m_N$ is replaced by the in-medium threshold $\sqrt{s_{1,\text{th}}^*}$. In line with equation (20), for the free non-resonant total cross sections $\sigma_{\pi'N \rightarrow NK^+K^-}^{\text{nr}}(\sqrt{s_1}, \sqrt{s_{1,\text{th}}})$ we have adopted the following expression:

$$\sigma_{\pi'N \rightarrow NK^+K^-}^{\text{nr}} \left(\sqrt{s_1}, \sqrt{s_{1,\text{th}}} \right) = \sigma_{\pi'N \rightarrow NK^+K^-} \left(\sqrt{s_1}, \sqrt{s_{1,\text{th}}} \right) - \sigma_{\pi'N \rightarrow N\phi} \left(\sqrt{s_1} \right) BR(\phi \rightarrow K^+K^-), \tag{33}$$

where $\sigma_{\pi'N \rightarrow NK^+K^-}(\sqrt{s_1}, \sqrt{s_{1,\text{th}}})$ are the corresponding total cross sections which include the contributions from ϕ and non- ϕ components, whereas $\sigma_{\pi'N \rightarrow N\phi}(\sqrt{s_1})$ are the total cross sections of the $\pi'N \rightarrow N\phi$ reactions. For the total cross sections $\sigma_{\pi'N \rightarrow NK^+K^-}(\sqrt{s_1}, \sqrt{s_{1,\text{th}}})$ and $\sigma_{\pi'N \rightarrow N\phi}(\sqrt{s_1})$ we have used in our model calculations the parametrizations (63) and (13) suggested in [43] and [60], respectively.

Before closing this subsection, one needs to define the exclusive differential cross section for the non-resonant K^+K^- production in pA interactions from the secondary processes (27), corresponding to the kinematical conditions of the ANKE experiment. Analogously to (23), the latter cross section can be determined as:

$$\begin{aligned}
& \frac{d\sigma_{pA \rightarrow K^+K^-X}^{\text{(sec)}} \left(\mathbf{p}_0, AW, p_{K^-} \right)}{dp_{K^+} d\Omega_{K^+} dp_{K^-} d\Omega_{K^-}} = \frac{1}{(2\pi)^2 (1 - \cos 12^\circ)^2} \frac{1}{0.4 \text{ GeV}/c} \\
& \times \int_{0.2 \text{ GeV}/c}^{0.6 \text{ GeV}/c} dp_{K^+} \int_{\cos 12^\circ}^1 d\cos\theta_{K^+} \int_{\cos 12^\circ}^1 d\cos\theta_{K^-} \int_0^{2\pi} d\phi_{K^+} \int_0^{2\pi} d\phi_{K^-}
\end{aligned} \tag{34}$$

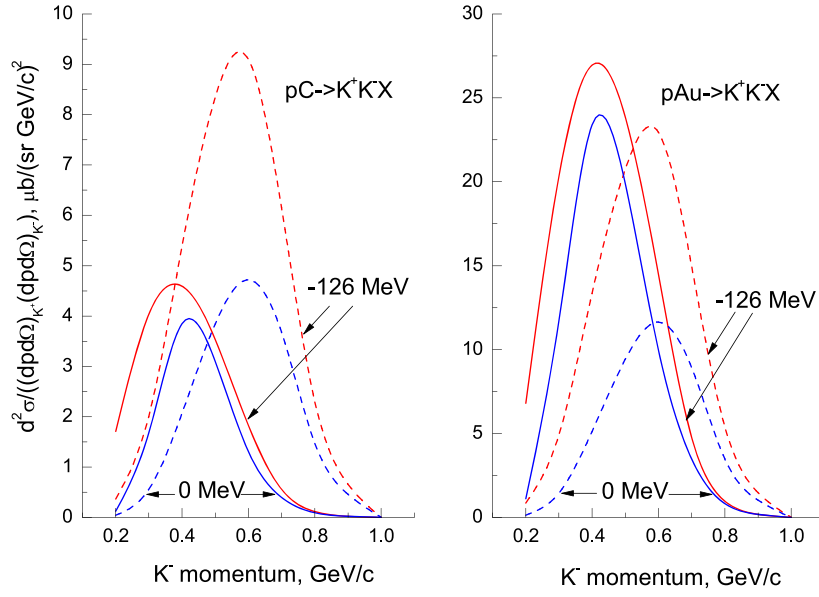


Figure 2. Exclusive differential cross section for the non-resonant production of K^+K^- pairs from primary and secondary channels (dashed and solid lines, respectively) in the ANKE acceptance window as a function of antikaon momentum in the interaction of protons of energy of 2.83 GeV with C (left panel) and Au (right panel) nuclei for K^- potential depths $U_{K^-}^0 = 0$ MeV and $U_{K^-}^0 = -126$ MeV as indicated by the curves.

$$\times \frac{d\sigma_{pA \rightarrow K^+K^-X}^{(\text{sec})}(\mathbf{p}_0, \mathbf{p}_{K^+}, \mathbf{p}_{K^-})}{d\mathbf{p}_{K^+} d\mathbf{p}_{K^-}} p_{K^+}^2 p_{K^-}^2 \theta[1.005 \text{ GeV} - IM(K^+K^-)],$$

where AW denotes ANKE acceptance window and it is defined above by the relations (24).

Let us discuss now the results of our calculations in the framework of the approach outlined above.

3. Results

First, we consider the non-resonant differential K^+K^- production cross sections in the ANKE acceptance window from the one-step and two-step creation mechanisms in pC and pAu collisions calculated on the basis of equations (23) and (34) for the proton kinetic energy of 2.83 GeV in two scenarios for the K^- potential depth $U_{K^-}^0$, namely: (i) $U_{K^-}^0 = 0$ MeV and (ii) $U_{K^-}^0 = -126$ MeV. In our calculations of these cross sections, presented in figure 2, the effective nuclear potentials $U_{K^+}^0$, U_N^0 as well as kaon, antikaon and proton Coulomb potentials, entering into the equation (5) determining the average in-medium hadron mass, were chosen equal to those introduced before and were retained to be fixed throughout the subsequent calculations reported below. One can see that the two-step K^+K^- production mechanism is of importance compared to the one-step in the chosen kinematics at laboratory antikaon momenta ≤ 0.4 GeV/c and ≤ 0.6 GeV/c for target nuclei C and Au, respectively, for both considered options for the K^- potential depth $U_{K^-}^0$, whereas at higher K^- momenta the direct K^+K^- production processes (1)–(4) are dominant and their dominance here is more

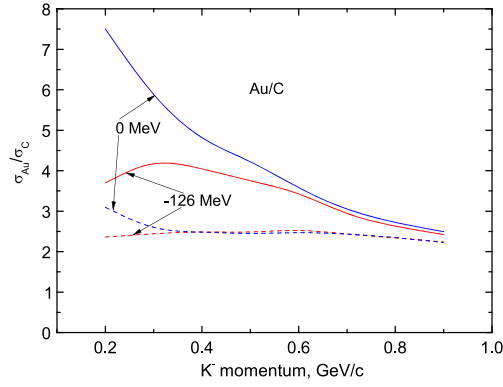


Figure 3. Ratio of the exclusive differential cross section for the non-resonant production of K^+K^- pairs off Au target nucleus in the ANKE acceptance window to that off C target nucleus as a function of antikaon momentum for the one-step and one-plus two-step K^+K^- production mechanisms (dashed and solid lines, respectively) for incident energy of 2.83 GeV as well as for K^- potential depths $U_{K^-}^0 = 0$ MeV and $U_{K^-}^0 = -126$ MeV as indicated by the curves.

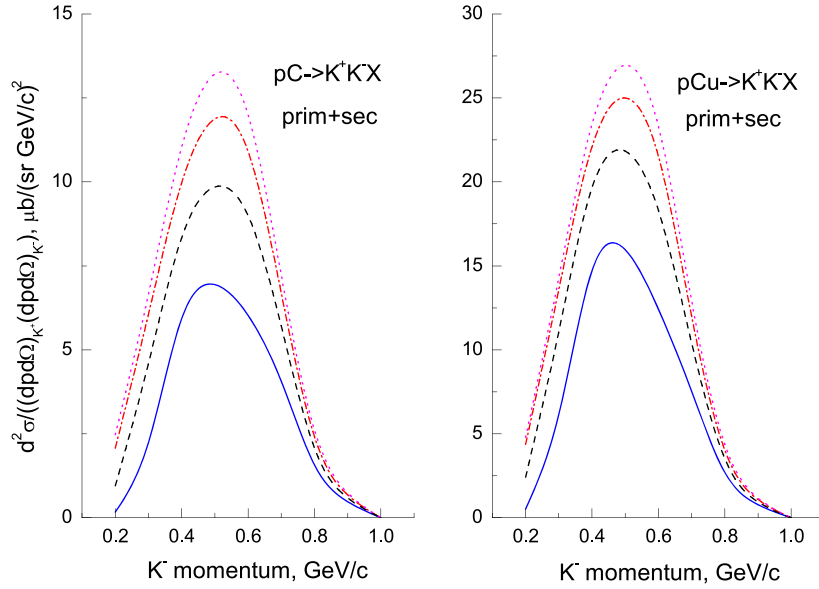


Figure 4. Exclusive differential cross section for the non-resonant production of K^+K^- pairs from primary plus secondary channels in the ANKE acceptance window as a function of antikaon momentum in the interaction of protons of energy of 2.83 GeV with C (left panel) and Cu (right panel) target nuclei for K^- potential depths $U_{K^-}^0 = 0$ MeV (solid lines), $U_{K^-}^0 = -60$ MeV (dashed lines), $U_{K^-}^0 = -126$ MeV (dotted-dashed lines) and $U_{K^-}^0 = -180$ MeV (dotted lines).

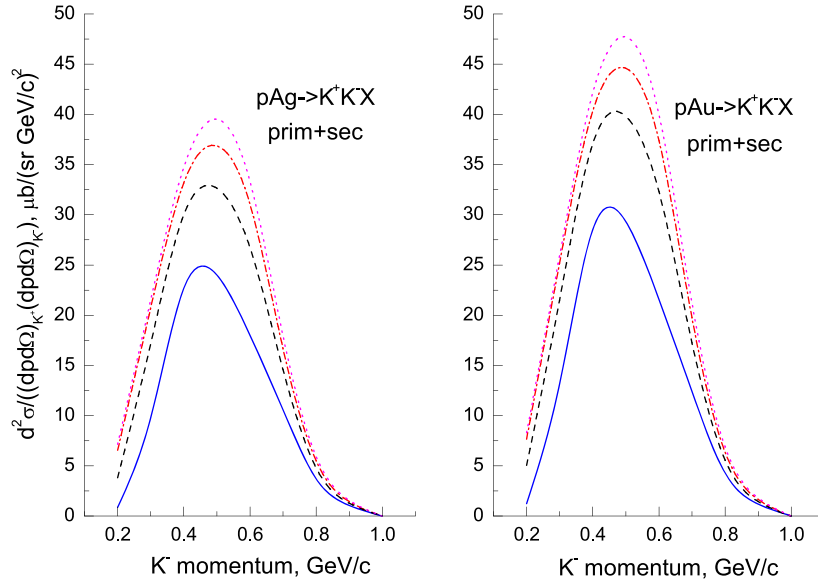


Figure 5. The same as in figure 4, but for the Ag and Au target nuclei.

pronounced, as is expected, for the carbon target nucleus. This indicates that the secondary pion–nucleon K^+K^- production channels have to be taken into account in the analysis of the data on non-resonant kaon pair creation in pA interactions obtained recently by the ANKE-at-COSY Collaboration. It is also clearly seen that the considered coincident antikaon spectrum from the one-step production mechanism reacts sensitively to the K^- potential practically at all antikaon momenta involved. The dependence of the K^- yield from the two-step production mechanism on this potential exists as well, but, contrary to the preceding case, it is more moderate. Therefore, as a result, the above offers the possibility to determine the antikaon potential experimentally (cf figures 4 and 5 given below).

In figure 3 we show our predictions for the another observable—the ratio of the exclusive differential cross section for the non-resonant production of K^+K^- pairs off Au target nucleus in the ANKE acceptance window to that off carbon target nucleus as a function of antikaon momentum for the one-step and one- and two-step kaon pair creation mechanisms for the projectile energy of 2.83 GeV and within the considered above two scenarios for the K^- potential depth $U_{K^-}^0$.¹⁸ It can be seen that there are essential differences between the results obtained by using different suppositions about the K^+K^- creation mechanism and the same potential depths $U_{K^-}^0$ (between solid and dashed lines). We may see, for example, that for low antikaon momenta, where the K^+K^- production via the secondary pion-induced reaction channels is enhanced, the calculated ratio can be of the order of 2.4 and 3.1 for the direct K^+K^- creation mechanism as well as 3.7 and 7.5 for the direct plus two-step K^+K^- production mechanisms when the antikaon potential depths of -126 and 0 MeV were applied,

¹⁸ It should be noticed that the similar inclusive observable was used in [8] and [11] in extracting the K^+ and K^0 nuclear potentials by comparing the inclusive data with the model calculations. Such relative observables are more favorable compared to those based on the absolute cross sections for the aim of getting the information on particle nuclear potential both from the experimental and theoretical sides, since, on the one hand, they allow for a reduction of systematic errors due to the cancellation of the efficiency corrections and, on the other hand, the theoretical uncertainties associated with the particle production and absorption mechanisms substantially cancel out in them.

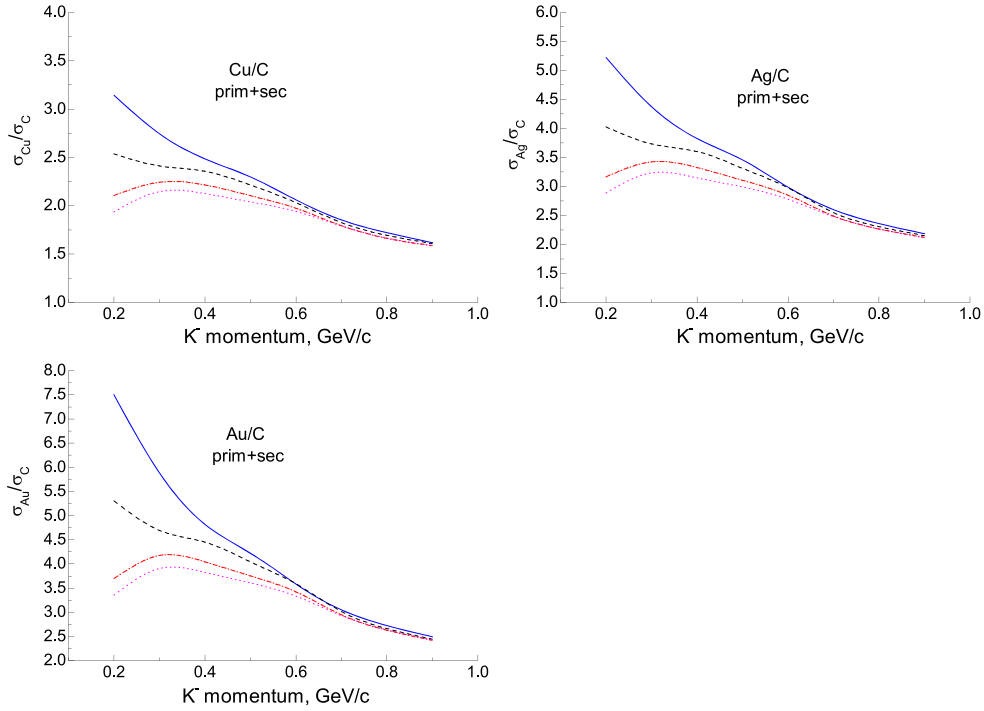


Figure 6. Ratio of the exclusive differential cross section for the non-resonant production of K^+K^- pairs off Cu, Ag and Au target nuclei presented in figures 4, 5 to that off C target nucleus given in figure 4 as a function of antikaon momentum for K^- potential depths $U_{K^-}^0 = 0$ MeV (solid lines), $U_{K^-}^0 = -60$ MeV (dashed lines), $U_{K^-}^0 = -126$ MeV (dotted-dashed lines) and $U_{K^-}^0 = -180$ MeV (dotted lines).

respectively. Therefore, we can conclude that in the analysis of data on this relative observable, taken in the ANKE experiment, it is important to account for the secondary pion-induced K^+K^- production processes. Looking at this figure, one can see also that the calculated ratio for the direct K^+K^- production mechanism, contrary to the absolute cross sections depicted in figure 2, is not very sensitive to the effective potential $U_{K^-}^0$, which is seen inside the nucleus by an antikaon, practically at all K^- momenta of interest. Whereas, this potential influences substantially the ratio of the differential cross sections under consideration obtained with accounting for the one- and two-step creation mechanisms, namely: the inclusion of the attractive K^- potential leads to the visible suppression of this ratio at low antikaon momenta (cf figure 6 given below). This leaves room for distinguishing between different K^- potentials from the measurements of the relative observable like that just considered.

Figures 4 and 5 show the results of our overall model calculations following equations (23) and (34) for the exclusive differential cross sections for the non-resonant production of K^+K^- pairs on C, Cu and Ag, Au target nuclei in the ANKE acceptance window for the primary and secondary K^+K^- creation processes obtained for bombarding energy of 2.83 GeV by employing in them four adopted options for the K^- potential depth $U_{K^-}^0$ to see more clearly the sensitivity of the calculated cross sections to the choice of the antikaon optical potential. It is nicely seen that for all nuclei there are measurable changes in the absolute cross sections for the K^+K^- production on these nuclei due to this potential,

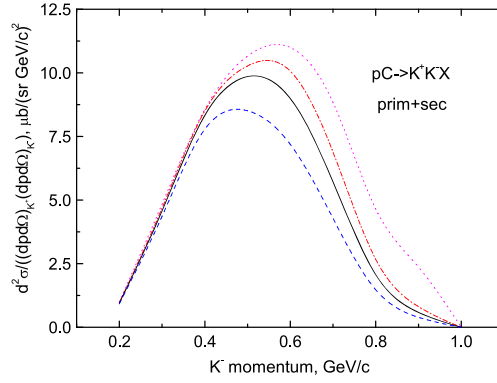


Figure 7. Exclusive differential cross section for the non-resonant production of K^+K^- pairs from primary plus secondary channels in the laboratory polar angular acceptance window $0^\circ \leq \theta_{K^\pm} \leq \theta_{\max}$ as a function of antikaon momentum in the interaction of protons of energy of 2.83 GeV with C target nucleus for K^- potential depth $U_{K^-}^0 = -60$ MeV and for $\theta_{\max} = 5^\circ$ (dotted line), $\theta_{\max} = 10^\circ$ (dotted-dashed line), $\theta_{\max} = 12^\circ$ (solid line), and $\theta_{\max} = 15^\circ$ (dashed line).

especially when it varies between -60 and 0 MeV (cf figure 2). We, therefore, can conclude that the K^- nuclear potential can be in principle extracted from the direct comparison of the results of our calculations, presented in figures 4 and 5, with the data from the ANKE experiment.

In figure 6 we show also the overall predictions of our model for the antikaon momentum dependence of the ratios of the exclusive differential cross sections for the non-resonant production of K^+K^- pairs off Cu, Ag and Au target nuclei, given, respectively, in figures 4 and 5, to that off C target nucleus, presented in figure 4, for four adopted options for the K^- potential depth $U_{K^-}^0$. One can see that the relative K^+K^- yield, along with the absolute one considered before, is appreciably sensitive to the antikaon potential at momenta less than 0.6 GeV/c for all considered A/C combinations, which is consistent with our previous findings of figure 3. Thus, our results demonstrate that the measurements of the K^- momentum dependence of the relative cross section for non-resonant K^+K^- production in pA collisions in the chosen kinematics and at beam energy of interest will also allow one to discriminate between four employed scenarios for the in-medium antikaon modification.

To extend the potential range of applicability of our model we performed calculations of the exclusive differential cross section for the non-resonant production of K^+K^- pairs from primary plus secondary channels for a carbon target nucleus in the scenario with K^- potential depth of -60 MeV at saturation density and for different polar angular acceptance windows for K^+ and K^- mesons. They are shown in figure 7. Here one can see a reduction of the cross section with respect to the case of $\theta_{\max} = 5^\circ$ with increasing the maximal angle of acceptance window θ_{\max} at antikaon momenta larger than 0.4 GeV/c¹⁹, whereas it is practically not changed at lower K^- momenta. Such behavior of the overall cross section of interest with increasing the K^\pm creation polar angular bin is expected to be observed both for other adopted options for antikaon potential depth $U_{K^-}^0$ and for other target nuclei considered in the present paper. It can be explained by the following. At low K^- momenta, the double differential cross

¹⁹ For example, the cross section is decreased by a factors of about 2 and 2.5 at momenta $\sim 0.7-0.8$ GeV/c when going from $\theta_{\max} = 5^\circ$ to $\theta_{\max} = 12^\circ$ and to $\theta_{\max} = 15^\circ$, respectively.

sections, appearing in equations (23) and (34) after averaging over the studied range of kaon momenta accounting for the kinematical constraint $IM(K^+K^-) \leq 1.005$ GeV depend weakly on the K^\pm production angles θ_{K^\pm} when they vary close to zero angle. Therefore, the integrals in formulas (23) and (34) are practically proportional to the solid angle, covered by the acceptance window, squared. Due to the employed definition of cross sections (23) and (34), this leads to a weak dependence of the overall exclusive cross section defined by these cross sections on the size of the acceptance window. At high K^- momenta, the reduction of the cross section with increasing this size is caused by the strong decrease of the above double differential cross sections with enlarging the K^\pm production angles θ_{K^\pm} . In view of the expected data from the ANKE experiment, the results presented in figure 7 can be also used as an additional tool to those given before for determining the K^- mean-field nuclear potential at studied range of antikaon momenta.

Taking into account the above considerations, we come to the conclusion that the absolute and relative observables such as the exclusive K^- momentum distribution and the ratio of this distribution on a heavy nucleus to that on a light one (C), considered in the present work, can be useful to help determine the antikaon–nucleus optical potential.

4. Conclusions

In this paper we calculated the antikaon momentum dependences of the exclusive absolute and relative non-resonant K^+K^- pair yields from pA ($A = \text{C, Cu, Ag and Au}$) collisions at 2.83 GeV beam energy in the acceptance window of the ANKE spectrometer, used in a recent experiment performed at COSY, by considering incoherent primary proton–nucleon and secondary pion–nucleon kaon pair production processes in the framework of a nuclear spectral function approach, which accounts for, in particular, nuclear mean-field potential effects on these processes. It was found that these observables are strongly sensitive to the antikaon–nucleus optical potential in the studied region of the antikaon momenta. This provides a nice opportunity to determine it from the direct comparison of the results of our calculations with the upcoming data from the ANKE-at-COSY experiment. It was also shown that the pion–nucleon production channels dominate in the low-momentum K^-, K^+ production in the considered kinematics and, therefore, they should be accounted for in the analysis of these data with the aim of obtaining information on the antikaon mean-field nuclear potential.

Acknowledgments

The authors gratefully acknowledge A Polyanskiy and H Ströher for their interest in this work.

References

- [1] Cassing W and Bratkovskaya E L 1999 *Phys. Rep.* **308** 65
- [2] Friedman E and Gal A 2007 *Phys. Rep.* **452** 89
- [3] Hartnack C *et al* 2012 *Phys. Rep.* **510** 119
- [4] Barth R *et al* 1997 *Phys. Rev. Lett.* **78** 4007
- Senger P 1996 (KaoS Collaboration) *Acta Phys. Pol. B* **27** 2993
- Sturm C *et al* 2001 *Phys. Rev. Lett.* **86** 39
- Shin Y *et al* 1998 *Phys. Rev. Lett.* **81** 1576

- Menzel M *et al* 2000 *Phys. Lett. B* **495** 26
Förster A *et al* 2003 *Phys. Rev. Lett.* **91** 152301
- [5] Herrmann N *et al* 1999 *Prog. Part. Nucl. Phys.* **42** 187
Ritman J L *et al* 1995 *Z. Phys. A* **352** 355
Crochet P *et al* 2000 *Phys. Lett. B* **486** 6
- [6] Büscher M *et al* 2004 *Eur. Phys. J. A* **22** 301
- [7] Li G Q, Lee C H and Brown G E 1997 *Phys. Rev. Lett.* **79** 5214
Li G Q, Lee C H and Brown G E 1999 *Nucl. Phys. A* **654** 523c
Larionov A B and Mosel U 2005 *Phys. Rev. C* **72** 014901
- [8] Rudy Z *et al* 2002 *Eur. Phys. J. A* **15** 303
Rudy Z *et al* 2005 *Eur. Phys. J. A* **23** 379
- [9] Schaffner-Bielich J, Mishustin I N and Bondorf J 1997 *Nucl. Phys. A* **625** 325
Li G Q, Ko C M and Fang X S 1994 *Phys. Lett. B* **329** 149
Korpa C L and Lutz M F M 2005 *Acta Phys. Hung. A* **22** 21
- [10] Zinyuk V *et al* 2014 *Phys. Rev. C* **90** 025210
- [11] Benabderrahmane M L *et al* 2009 *Phys. Rev. Lett.* **102** 182501
- [12] Agakishiev G *et al* 2010 *Phys. Rev. C* **82** 044907
Agakishiev G *et al* 2014 *Phys. Rev. C* **90** 054906
- [13] Lutz M 1998 *Phys. Lett. B* **426** 12
- [14] Schaffner-Bielich J, Koch V and Effenberger M 2000 *Nucl. Phys. A* **669** 153
- [15] Ramos A and Oset E 2000 *Nucl. Phys. A* **671** 481
- [16] Cieply A *et al* 2001 *Nucl. Phys. A* **696** 173
- [17] Ramos A *et al* 2001 *Nucl. Phys. A* **691** 258
- [18] Tolos L, Ramos A and Oset E 2006 *Phys. Rev. C* **74** 015203
- [19] Tolos L, Cabrera D and Ramos A 2008 *Phys. Rev. C* **78** 045205
- [20] Tolos L, Ramos A, Polls A and Kuo T T S 2001 *Nucl. Phys. A* **690** 547
- [21] Tolos L, Ramos A and Polls A 2002 *Phys. Rev. C* **65** 054907
- [22] Friedman E, Gal A and Batty C J 1993 *Phys. Lett. B* **308** 6
Friedman E, Gal A and Batty C J 1994 *Nucl. Phys. A* **579** 518
- [23] Friedman E, Gal A, Mares J and Cieply A 1999 *Phys. Rev. C* **60** 024314
- [24] Cieply A *et al* 2011 *Phys. Rev. C* **84** 045206
- [25] Gal A 2013 *Nucl. Phys. A* **914** 270
Gal A *et al* 2014 *EPJ Web Conferences* **81** 01018
- [26] Akaishi Y and Yamazaki T 2002 *Phys. Rev. C* **65** 044005
Akaishi Y, Dote A and Yamazaki T 2005 *Phys. Lett. B* **613** 140
- [27] Suzuki T *et al* 2004 *Phys. Lett. B* **597** 263
Suzuki T *et al* 2005 *Nucl. Phys. A* **754** 375c
- [28] Agnello M *et al* 2005 *Phys. Rev. Lett.* **94** 212303
Agnello M *et al* 2006 *Nucl. Phys. A* **775** 35
Agnello M *et al* 2007 *Phys. Lett. B* **654** 80
- [29] Yamazaki T *et al* 2010 *Phys. Rev. Lett.* **104** 132502
- [30] Fabbietti L *et al* 2013 *Nucl. Phys. A* **914** 60
Epple E (HADES Collaboration) 2013 arXiv: 1304.5896
Agakishiev G *et al* 2015 *Phys. Lett. B* **742** 242
- [31] Sato M *et al* 2008 *Phys. Lett. B* **659** 107
- [32] Hashimoto T *et al* 2014 arXiv: 1408.5637
- [33] Ichikawa Y *et al* 2014 arXiv: 1411.6708
- [34] Oset E and Toki H 2006 *Phys. Rev. C* **74** 015207
Ramos A, Magas V K, Oset E and Toki H 2007 *Eur. Phys. J. A* **31** 684
Magas V K, Oset E and Ramos A 2008 *Phys. Rev. C* **77** 065210
Ramos A, Magas V K, Oset E and Toki H 2007 arXiv: nuclth/0702019
Magas V K, Ramos A, Yamagata-Sekihara J, Hirenzaki S and Oset E 2009 *Nonlinear Phenom. Complex Syst.* **12** 414
- [35] Kishimoto T *et al* 2007 *Prog. Theor. Phys.* **118** 181
Kishimoto T *et al* 2009 *Nucl. Phys. A* **827** 321c
- [36] Scheinast W *et al* 2006 *Phys. Rev. Lett.* **96** 072301
- [37] Akindinov A V *et al* 2010 *J. Phys. G: Nucl. Part. Phys.* **37** 015107
- [38] Akindinov A V *et al* 2007 *JETP Lett.* **85** 142

- [39] Sibirtsev A and Cassing W 1999 arXiv: [nuclth/9909053](#)
- [40] Polyanskiy A *et al* 2011 *Phys. Lett. B* **695** 74
- [41] Hartmann M *et al* 2012 *Phys. Rev. C* **85** 035206
- [42] Maeda Y *et al* 2009 *Phys. Rev. C* **79** 018201
- [43] Paryev E Y 2000 *Eur. Phys. J. A* **9** 521
- [44] Paryev E Y 2005 *Eur. Phys. J. A* **23** 453
- [45] Paryev E Y 2013 *J. Phys. G: Nucl. Part. Phys.* **40** 025201
- [46] Magas V K *et al* 2010 *Phys. Rev. C* **81** 024609
- [47] Lee C H *et al* 1997 *Phys. Lett. B* **412** 235
- [48] Paryev E Y 2009 *J. Phys. G: Nucl. Part. Phys.* **36** 015103
- [49] Efremov S V and Paryev E Y 1994 *Z. Phys. A* **348** 217
- [50] Maeda Y *et al* 2008 *Phys. Rev. C* **77** 015204
- [51] Ye Q J *et al* 2012 *Phys. Rev. C* **85** 035211
- [52] Ye Q J *et al* 2013 *Phys. Rev. C* **87** 065203
- [53] Li G Q, Lee C-H and Brown G E 1997 *Nucl. Phys. A* **625** 372
- [54] Sibirtsev A and Cassing W 1998 *Nucl. Phys. A* **641** 476
- [55] Balestra F *et al* 2001 *Phys. Rev. C* **63** 024004
- [56] Quentmeier C *et al* 2001 *Phys. Lett. B* **515** 276
Winter P *et al* 2006 *Phys. Lett. B* **635** 23
Silarski M *et al* 2009 *Phys. Rev. C* **80** 045202
- [57] Yao T 1962 *Phys. Rev.* **125** 1048
- [58] Sibirtsev A, Cassing W and Ko C M 1997 *Z. Phys. A* **358** 101
- [59] Kaptari L P and Kämpfer B 2005 *Eur. Phys. J. A* **23** 291
- [60] Sibirtsev A 1996 *Nucl. Phys. A* **604** 455